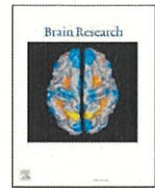学 位 論 文

Ascending spinal tract formation in chick embryo originating from different spinal regions.

香川大学大学院医学系研究科

医学専攻

國土 曜平

Contents lists available at ScienceDirect

Brain Research

Ascending spinal tract formation in chick embryo originating from different spinal regions

Yohei Kokudo [a], Takahiro Arakawa [b], Hiroo Takahashi [b], Hideki Kobara [c], Masaki Kamada [a], Kazushi Deguchi [c], Tetsuo Touge [d], Tsutomu Masaki [c], Tohru Yamamoto [b,*]

[a] Department of Neurological Intractable Disease Research, Faculty of Medicine, Kagawa University, Kagawa 761-0793, Japan
[b] Department of Molecular Neurobiology, Faculty of Medicine, Kagawa University, 761-0793, Japan
[c] Department of Gastroenterology and Neurology, Faculty of Medicine, Kagawa University, Kagawa 761-0793, Japan
[d] Department of Gastroenterology and Neurology, Faculty of Medicine, Kagawa University, Kagawa 761-0793, Japan

ARTICLE INFO

ABSTRACT

The present study aimed to assess spinal tract formation in neurons originating from cervical (C7), brachial (C14), and thoracic (T4) regions, with the lumbar (LS2) region as a reference, in a chick embryo. For the assessment of the spinal tracts, we introduced a vector expressing human placental alkaline phosphatase into progenitor cells generated after neural tube closure and belonging to the above segments, using in ovo electroporation. The ascending axons took primarily similar paths: dorsal commissural, ventral commissural, and dorsal non-commissural paths, with some variance depending on their originating segments. Some populations of non-commissural neurons later extended their axons following a ventral path. The elongation rates of these axons are primarily constant and tended to increase over time; however, some variations depending on the originating segments were also observed. Some of the dorsally ascending axons entered into the developing cerebellum, and spinocerebellar neurons originating from T4 projected their axons into the cortex of the cerebellum differently from those from LS2. These results unveil an overall picture of early ascending spinal tract formation.

1. Introduction

The spinal cord is a path that connects the central command and peripheral information and contains neurons that serve as relay points for particular commands and/or information. Spinal neurons involved in communicating peripheral information to an upper command center send their axons anteriorly to reach certain commanding centers and/or other relay points. The generation of spinal neurons and their resultant connections, such as spinocerebellar, spinothalamic, spinoreticular, spinotectal, and spino-olivary tracts, are well studied and described (reviewed in Sagner and Briscoe, 2019; Watson and Harrison, 2012). However, little is known about their formation during the development of the spinal cord.

We developed a method for labeling a single segment-derived spinal neuron generated after neural tube closure by in ovo electroporation and reported the early ascending tract formation originating from lumbo-sacral 2 spinal segment (LS2) (Arakawa et al., 2008). However, the spinal cord consists of four regions (cervical, brachial, thoracic, and lumbosacral), which have different properties primarily due to their corresponding spinal neurons being in charge of different tissues. It is not clear if the formation of the ascending tracts originating from these different spinal regions is the same as in those originating from LS2. Whether these ascending tract neurons send their axons in the same way to reach their destinations remains unknown.

To resolve the above issues, we observed the formation of ascending tracts originating from different spinal regions: cervical 7 (C7) belonging to the cervical region, cervical 14 (C14) belonging to the brachial region, and thoracic 4 (T4) belonging to the thoracic region, with LS2 as a reference.

2. Results

2.1. Formation of ascending spinal tracts originating from cervical, brachial, thoracic, and lumbosacral regions in chick embryo

To investigate ascending spinal tract formation in regions other than

---

the lumbosacral, in particular the cervical, brachial, and thoracic regions, we unilaterally electroporated human placental alkaline phosphatase (PLAP)-expressing vectors in the neural progenitors of C7 (cervical), C14 (brachial), and T4 (thoracic) segments at Hamburger-Hamilton stage (Hamburger and Hamilton, 1951) 12 (HH12), HH14, and HH16, respectively. These stages were chosen for adjusting the time of electroporation after neural tube closure in each segment to that of LS2 at HH18 (*ca.* 10–14 h after neural tube closure; Hamburger and Hamilton, 1951). We also electroporated the vector at LS2 as a reference for the following experiments, the results of which are shown. In electroporation *in ovo*, some populations of neurons may fail to be labeled and are therefore overlooked; however, the labeled progenitors were evenly distributed along dorso-ventral axis after electroporation in our experimental conditions (Arakawa et al., 2008), indicating that the resultant images represent the major axons originating from neurons generated at the indicated segments, during and soon after electroporation. Each electroporated embryo was dissected at HH25, HH26, HH27, or HH28. The expression of the electroporated PLAP was fairly restricted within the indicated single segments, except in C7, where it tended to expand beyond the segment boundaries (Fig. 1).

Ascending commissural axons originating from each segment were observed by HH25 (Fig. 2). Axons originating from C14 and T4 followed two major pathways, relatively dorsal and ventral pathways, similar to those observed in LS2 (Arakawa et al., 2008). A small population of axons from LS2 extended between these dorsal and ventral pathways, as observed previously; however, axons from T4 rarely took that intermediate path. In the ascending axons from C14, a small population tended to extend between dorsal and ventral pathways resembling the observed in LS2 commissural axons; however, they appeared to later join the dorsal pathway. Ascending axons originating from C7 appeared to primarily follow a dorsal pathway in a relatively diffuse manner, and some axons seemed to take a more ventral path.

Ascending non-commissural axons originating from each segment could also be observed around HH25-26 (Fig. 2). These axons traveled the dorsal pathway to the medulla oblongata, as observed in those from LS2. However, a discernible population of axons taking a ventral pathway later appeared around HH28 and became more evident at HH29 including those originating from LS2 (Supplemental Fig. 3).

To precisely see the positions of the paths, some of HH28 spinal cords were prepared in an 'open-book' configuration (Supplemental Fig. 1).

Both commissural and non-commissural dorsally ascending axons traveled around the middle of the spinal cord, and those ventrally ascending axons traveled in proximity to the floor plate, with no apparent difference among the originating segments. We further prepared coronal section of HH28 spinal cords at T5, of which ascending axons originating from LS2, at T2, of which ascending axons originating from T4, at C10, of which ascending axons originating from C14, and at C3, of which ascending axons originating from C7 were visualized, to define the positions of dorsal, ventral, and intermediate paths (Supplemental Fig. 2). The dorsal paths appeared beneath the dorsal root entry zone, the ventral paths appeared in proximity to the floor plate, and the intermediate paths originating from LS2 appeared in-between the dorsal and ventral paths.

Both commissural and non-commissural ascending axons entered the medulla oblongata around HH29-30 (Fig. 3). Some of the dorsally ascending axons originating from T4 and C14 (and scarcely from C7) bifurcated to approach the cerebellum, as observed in those originating from LS2. The majority of the remaining ascending axons entered the superior medullary velum. Axons extending further were rarely observed under our experimental conditions. Non-commissural axons taking the ventral path that appeared later in C7, C14, and T4 reached the medulla oblongata by HH30 (originating from C7 or C14) or HH33 (originating from T4). Non-commissural ventral axons originating from LS2 did not reach the medulla oblongata at HH30, and their presence became hardly discernible from other broadened, dorsally running axons beyond HH33.

2.2. Elongation rates of ascending axons vary during their development

The ascending axon elongation time course according to the origin region (C7, C14, and T4, with LS2 as a reference) is schematically represented in Fig. 4A. The axons from these regions appeared to constantly elongate; however, their elongation varied. For example, the commissural axons originating from T4 first appeared to lead the axons from LS2, but LS2 axons later reached T4 axons around the brachial region, and both commissural axons reached the medulla oblongata by HH30. We next verified if these variations in elongation were due to differences in elongation rates. Considering that cell bodies responsible for the elongation of these axons are located in a single segment area, we can estimate axon elongation rates at each developmental stage with single
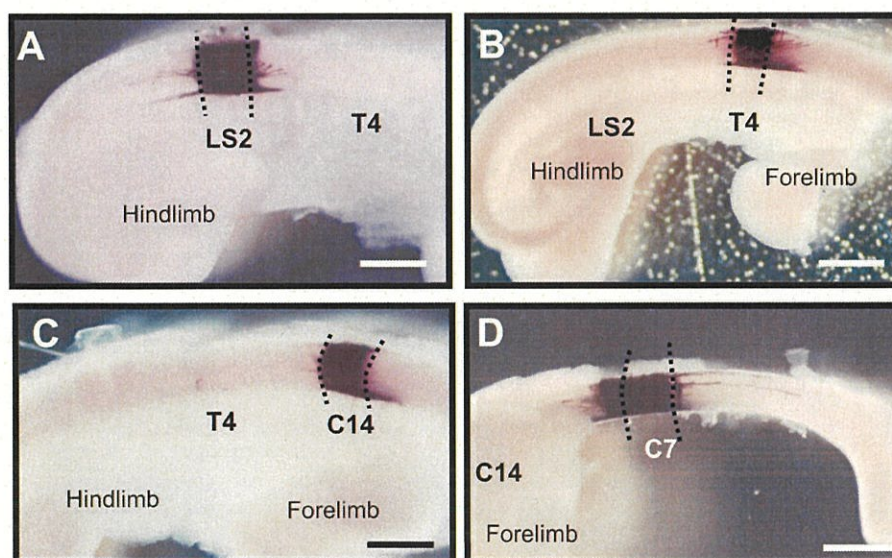

Fig. 1. Expression of PLAP at HH25. (A) Introduced in LS2 at HH18, (B) in T4 at HH16, (C) in C14 at HH14, and (D) in C7 at HH12 by *in ovo* electroporation. The expression of hPLAP is fairly limited within the indicated single segment except for C7, which tended to expand its expression beyond the segment boundaries. Scale bar = 1 mm.
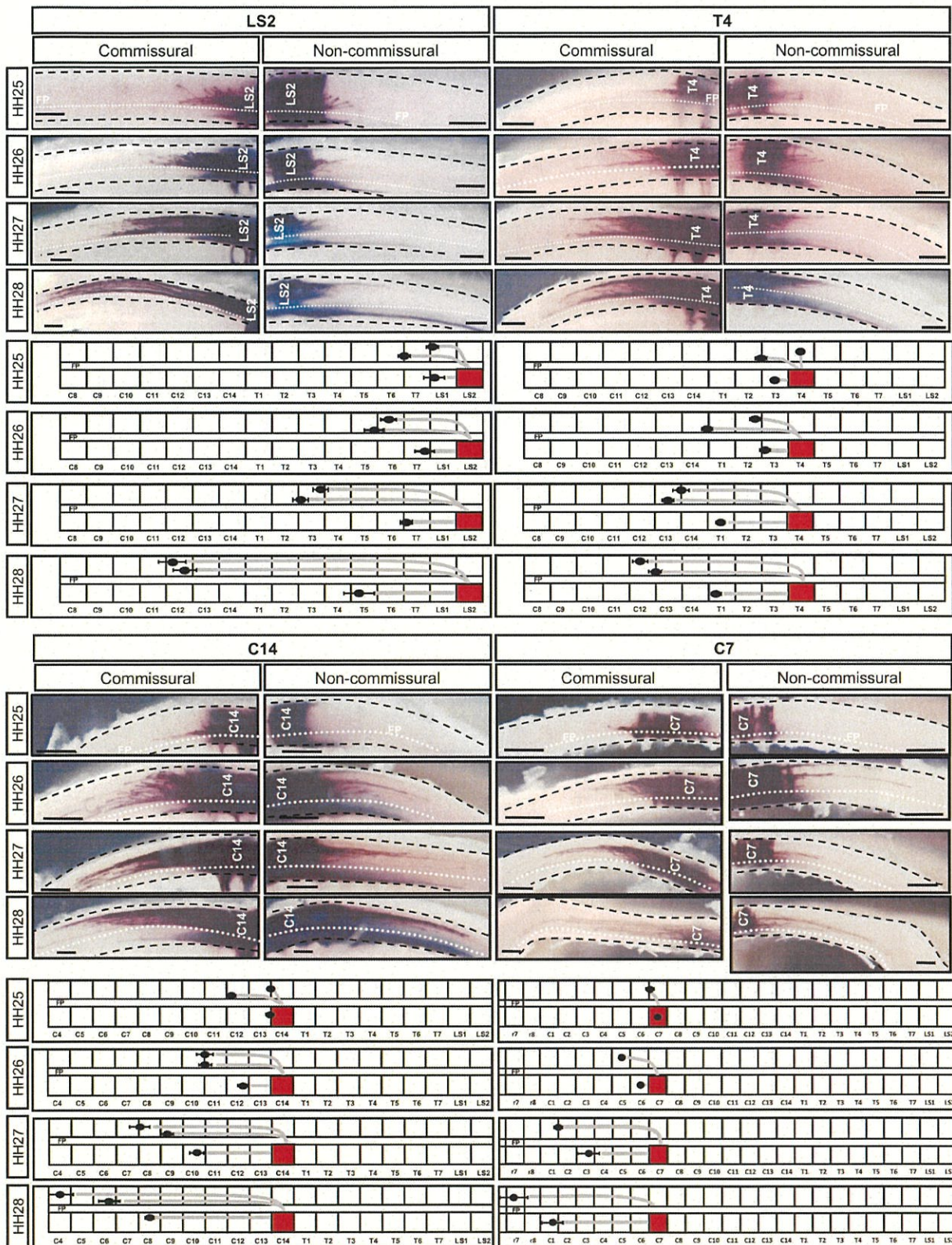
Fig. 2. Commissural and non-commissural ascending axons originating from LS2, T4, C14, and C7. The positions of the observed axon tips are also schematically summarized (error bars: standard error of mean). The position of the floor plate is indicated by the white dotted line. The spinal cord is outlined by the black dashed lines. LS2: HH25, n = 5; HH26, n = 11; HH27, n = 12; HH28, n = 10, T4: HH25, n = 6; HH26, n = 10; HH27, n = 9; HH28, n = 9, C12: HH25, n = 8; HH26, n = 8; HH27, n = 12; HH28, n = 10, C7: HH25, n = 4; HH26, n = 4; HH27, n = 3; HH28, n = 4. Scale bar = 0.5 mm.
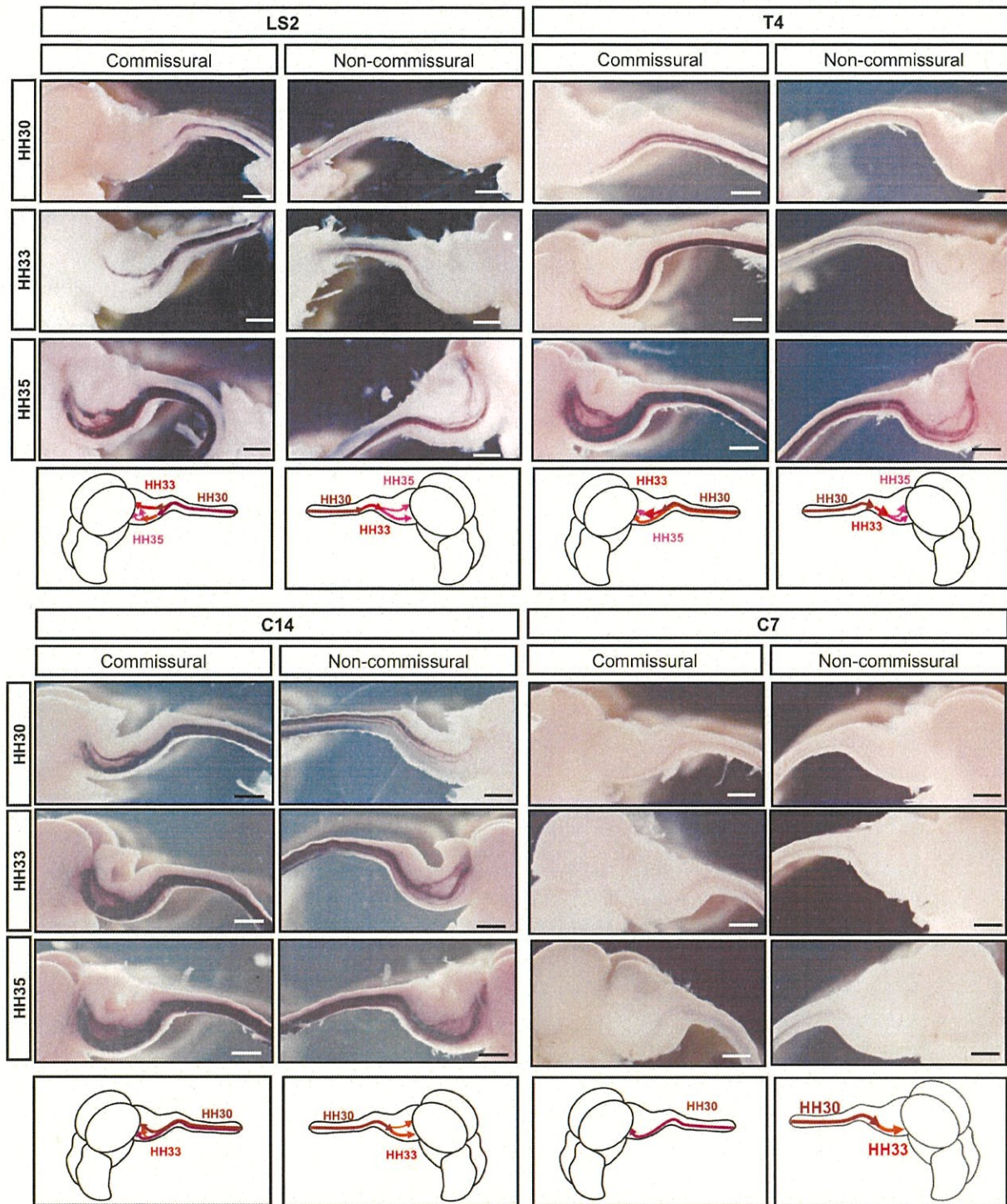
Fig. 3. Commissural and non-commissural ascending axons originating from LS2, T4, C14, and C7 in the medulla oblongata and a schematic representation. LS2: HH30, n = 6; HH33, n = 10; HH35, n = 5, T4: HH30, n = 4; HH33, n = 7; HH35, n = 6, C12: HH30, n = 13; HH33, n = 10; HH35, n = 5, C7: HH30, n = 6; HH33, n = 5; HH35, n = 6. Scale bar = 1 mm.

segment-length accuracy. To calculate the elongation rates, we first measured the average length of each segment of the spinal cord and rhombomere from HH26, HH27, HH28, and HH30 embryos. We plotted the positions of most axon tips and calculated the distance from the average positions at previous stages. As shown in Fig. 4B, initial elongation rates of ascending axons (50–100 μm/h) are primarily constant

and tended to mildly accelerate; however, axons originating from some segments behaved differently at certain stages. For example, the elongation rates of commissural and non-commissural axons originating from LS2 significantly augmented at HH28 (commissural dorsal: p < 0.001; commissural ventral: p = 0.006; non-commissural: p = 0.049). On the contrary, those from T4 were rather constant (commissural) or
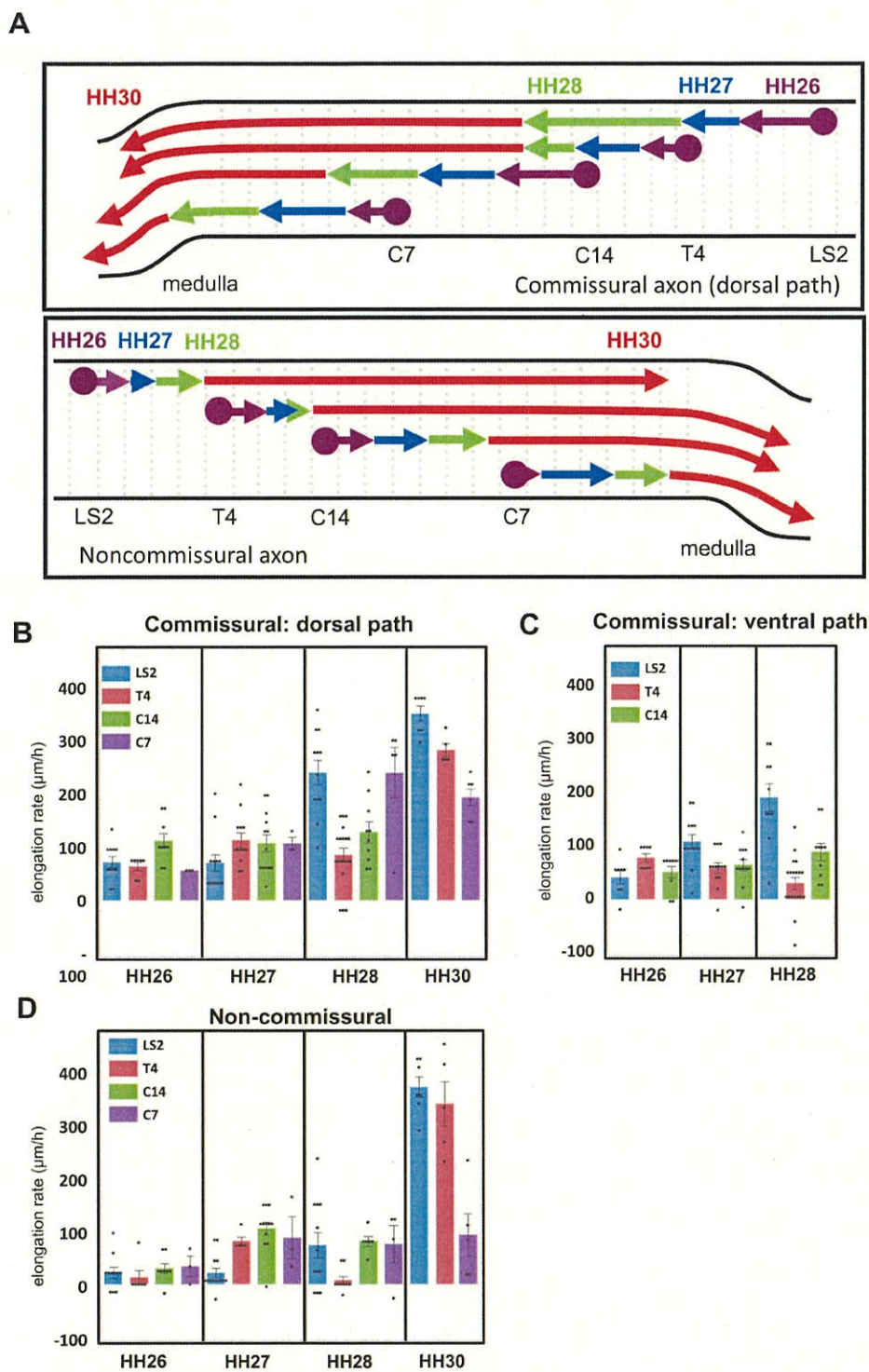
Fig. 4. (A) Schematic representation of the paths and elongation time courses of ascending axons originating form lumbosacral (LS2), thoracic (T4), brachial (C14), and cervical (C7) regions. (B-D) Elongation rates (μm/h) of LS2 (blue), T4 (red), C14 (green), and C7 (purple) derived-ascending axons taking commissural dorsal (B), commissural ventral (C), and non-commissural dorsal (D) paths. Error bars represent standard error of the mean.

even decreased (non-commissural: p < 0.001). As a result, commissural axons originating from LS2 caught up with those originating from T4 around brachial region. After passing through the brachial region, these commissural axons originating from different spinal segments reached medulla oblongata at similar timing with comparable elongation rates. These observations suggest that the elongation rates of ascending axons

are differently regulated according to their origins.

2.3. Spinocerebellar axons originating from C14, T4, and LS2 differently project into the developing cerebellum

Some of the dorsally ascending axons originating from T4 and C14

(and barely from C7) bifurcated to approach the cerebellum, as observed in those originating from LS2. These axons entered the developing cerebellum by HH33 (Fig. 5). The rarely observed spinocerebellar commissural axons originating from C7 became vague for proper evaluation beyond this stage. Commissural spinocerebellar axons entered earlier into the cerebellum than non-commissural axons, and commissural spinocerebellar axons already re-crossed (LS2) or re-crossing (C7, C14, and T4) the midline were visible at HH33. Spinocerebellar axons originating from LS2 appeared to take dorsal-most path, entered into developing cerebellum, and re-crossed the midline (Supplemental

Fig. 4) to reach lobules II–III with a characteristic projection pattern, as previously reported (Arakawa et al., 2008). The spinocerebellar axons originating from T4 became rarely detectable from the outside because of the enlarged developing cerebellum, and became visible again in their projection to lobule III (Fig. 5). Spinocerebellar axons originating from C14 stayed at the bottom of the cerebellum and became rarely visible outside of it after HH36. These observations indicated that the projection of spinocerebellar axons was differently regulated to produce several specific projection patterns in the cerebellum according to the spinal segment of origin.
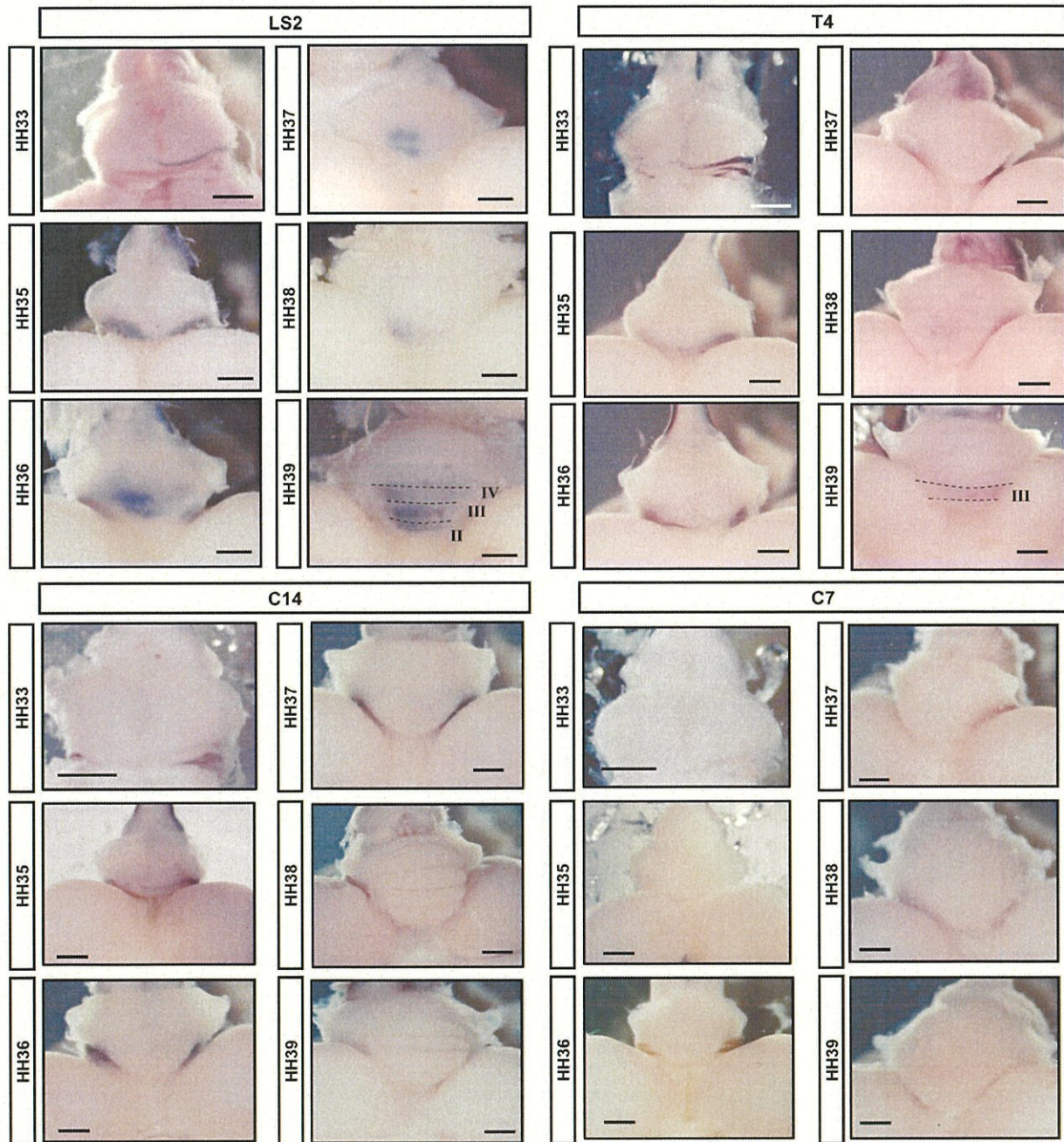

Fig. 5. Ascending axons originating from LS2, T4, C14, and C7 entering the developing cerebellum, and their projections in the developing cerebellum. LS2: HH33, n = 5; HH35, n = 7; HH36, n = 13; HH37, n = 7; HH38, n = 5; HH39, n = 15, T4: HH33, n = 6; HH35, n = 12; HH36, n = 3; HH37, n = 4; HH38, n = 6; HH39, n = 7, C12: HH33, n = 5; HH35, n = 7; HH36, n = 13; HH37, n = 7; HH38, n = 5; HH39, n = 15, C7: HH33, n = 6; HH35, n = 12; HH36, n = 3; HH37, n = 4; HH38, n = 6; HH39, n = 7. Scale bar = 1 mm.

3. Discussion

Here, we describe the formation of spinal ascending tracts originating from single segments belonging to different regions: cervical (C7), brachial (C14), thoracic (T4), and lumbar (LS2). Their characteristics were similar: all formed commissural and non-commissural pathways; commissural neurons ascended through two major pathways, a dorsal and a ventral pathway, and non-commissural neurons ascended primarily through a dorsal pathway, and some populations subsequently followed a ventral pathway. Their elongation rates varied depending on their origins and developmental stages. They reached the medulla oblongata by HH30-33, and some axons of the dorsal pathway entered the developing cerebellum. Commissural axons that entered the cerebellum re-crossed the midline and extended with non-commissural axons in a particular manner depending on their originating spinal segment.

Ascending axons originating from different regions primarily took similar paths; however, those from C7, C14, and T4 showed different behavior than LS2-derived ascending neurons. For example, a minor but easily identifiable population of commissural axons followed an intermediate path between the major dorsal and ventral paths in LS2-derived ascending neurons. However, commissural neurons originating from C7 or T4 rarely followed such intermediate path. A small population of neurons originating from C14 tended to extend their axons between the dorsal and ventral pathways, but later appeared to join the dorsal pathway. These observations indicate that different spinal neurons exist in a given spinal region and/or segment.

In our study, neurons originating from C7 rarely entered the cerebellum, and spinocerebellar neurons originating from C14 did not appear to project their axons into the cerebellar cortex. It has been reported that spinocerebellar neurons originate in the brachial and cervical regions in chicks (Okado et al., 1987; Furue et al., 2010), cats (Yaginuma and Matsushita, 1986; Matsushita and Tanami, 1987), and mice (Baek et al., 2019; Coughlan et al., 2019), indicating that spinocerebellar neurons should exist in these regions. This inconsistency may be due to inefficient labeling of later-born neurons, which may be a major source of spinocerebellar neurons derived from these segments. We tried incorporating the PLAP vector into the neuron progenitor genome using transposase (Tol2 or PiggyBac); however, this did not alter the results described above, although spinocerebellar axons were visible at later stages in embryos where PLAP vector was incorporated into the genome with transposases (Supplemental Fig. 5). It was also difficult to electroporate vectors into a single spinal segment of C7 in older embryos because of flexure with thickened tissue around the cervical region. Further analyses with improved methodology are needed to visualize the process of spinocerebellar tract formation derived from single spinal segments of the cervical and brachial regions.

We limited the regions where the PLAP-expressing vector was incorporated around a single segment, which enabled us to estimate their axon elongation rates at each developmental stage in single segment-length accuracy. Most commissural ascending axons initially elongated at 50–100 μm/h and tended to increase their elongation rates later. However, later-born LS2-derived dorsal commissural axons significantly boosted their elongation rate at HH27–28 and reached the earlier-born T4-derived axons. After passing the brachial region, elongation rate of T4-derived commissural axons also boosted to ~300 μm/h, comparable to those of LS2-derived axons, and they reached the medulla oblongata and some entered the developing cerebellum at roughly the same time period. Ventrally running commissural neurons also exhibited similar trends in axon elongation rate. The functional relevance of the observed acceleration differences of commissural neurons is not clear; however, the fact that axons of spinocerebellar neurons originating from different segments entered the developing cerebellum at roughly the same time might indicate that axons need to reach the cerebellum, as well as other destinations, within a given developmental time period. Such a short time period might be needed for them to re-

cross the midline in the developing cerebellum. Since non-commissural ascending axons did not show such regulated elongation, LS2-derived non-commissural spinocerebellar neurons entered the cerebellum later, following T4-derived spinocerebellar neurons that did not re-cross the midline to project their axons to the ipsilateral side of the cerebellum. Concerning the midline re-crossing of commissural spinocerebellar neurons in the cerebellum, LS2-derived neurons reached and re-crossed the midline by HH33, and the corresponding neurons originating from another spinal region crossed after HH33. LS2-derived commissural spinocerebellar neurons robustly extended their axons onto the developing cerebellar cortex; however, other segment-derived re-crossed neurons maintained their axons underneath the cortex, and some T4-derived axons appeared around the cortex later, at HH38. Further analyses are needed to clarify the functional significance of the variety of ascending axon behaviors and mechanisms contributing to such differences in region-derived ascending tract neurons.

Here, we analyzed ascending spinal tract formation immediately after neural tube closure in developing chick embryos. In conclusion, we confirmed that the ascending paths taken by axons originating from single segments belonging to different regions (C7, C14, T4, and LS2) are essentially the same; however, their elongation and cerebellar projection profiles are different, which supposedly reflects their regional identities. Our findings clearly reflect the differences in the behavior of the axons projecting into the cerebellum, which could be utilized to verify the underlying mechanism that governs the antero-posterior identity of spinocerebellar neurons. We observed formation of ascending spinal tracts that would include several species of neurons of which destinations are different; however, our analyses provide a developmental and anatomical basis for further investigations aimed at elucidating the underlying mechanisms of ascending spinal tract formation.

4. Experimental procedures

4.1. Construction of expression vectors

The PLAP expression vector was constructed as previously described (Arakawa et al., 2008). To integrate the expression vector into the genome with Tol2 transposase, PLAP cDNA was inserted into the *XbaI-EcoRV* site of pT2K-CAG-EGFP (Sato et al., 2007; gift from Yoshiko Takahashi at Kyoto University).

4.2. In ovo electroporation

In ovo electroporation into a single spinal segment was performed as previously described (Arakawa et al., 2008). The solution containing the PLAP expression vector (3 μg/μl in Tris-EDTA pH 7.4) was injected into the central canal around C7, C14, T4, or LS2 at HH12, HH14, HH16, or HH18, respectively, and electroporated with the electrode (0.15 mm in length; BEX CO, LTD, Japan). For electroporation at HH12, 10 μl of neutral red (10 mg/ml, Invitrogen) was applied to the embryo to visualize somites. For electroporating PLAP with *Hox*-expressing vectors, a hPLAP expression vector (1.5 μg/μl) and *Hox* expression vector (1.5 μg/μL) mixture was injected into the central canal and co-electroporated with a larger electrode (1 mm in length). The work described here was carried out in accordance with The Code of Ethics of the World Medical Association (Declaration of Helsinki) for experiments involving humans http://www.wma.net/en/30publications/10policies/b3/index.html; EC Directive 86/609/EEC for animal experiments http://ec.europa.eu/environment/chemicals/lab_animals/legislation_en.htm; Uniform Requirements for manuscripts submitted to Biomedical journals http://www.icmje.org.

4.3. Whole mount alkaline phosphatase activity staining

Whole mount alkaline phosphatase activity staining was performed

as previously described (Arakawa et al., 2008). Briefly, the dissected embryos were fixed, washed, and incubated at 65 °C in PBS for 8 to 16 h to inactivate the endogenous alkaline phosphatase (AP) activity. Residual AP activity was visualized by incubating the embryos with NBT/BCIP (Roche) in 100 mM Tris–Cl (pH 9.5) containing 100 mM NaCl and 50 mM $MgCl_2$ at 4 °C for 24 h. For quantification of stained axons appearing on the developing cerebellum at HH36, the images were turned to grey scale with ImageJ software, and intensities from each pixel in the anterior hemispheres around lobules II-III were summed after subtracting background intensities around the center of lobule VI with ImageJ software.

4.4. Analysis of the elongation rate of ascending spinal neurons

The positions of the ascending axonal tips were recorded. Fixed HH26 (n = 8), HH27 (n = 5), HH28 (n = 6), and HH30 (n = 5) embryos were dissected to measure average segment lengths in different spinal regions and developmental stages. The lengths from the originating segments were calculated according to the diagrams obtained above, and the elongation speeds at each stage were calculated by dividing the length of elongation from the average of the previous stage by the average of hours needed to reach the actual stage from the previous one.

4.5. Statistical analyses

Data are expressed as means ± S.E. Statistical differences were assessed using unpaired two-tailed Student's t tests for two comparisons, and non-parametric one-way non-repeated measures ANOVA with Dunnett's post hoc test for multiple comparisons. A p value of <0.05 was considered statistically significant. No sample size calculation, tests for normal distribution, or tests for outliers were performed.

CRediT authorship contribution statement

Yohei Kokudo: Methodology, Formal analysis, Investigation, Writing – original draft. **Takahiro Arakawa:** Methodology, Formal analysis, Investigation. **Hiroo Takahashi:** Methodology, Formal analysis, Investigation. **Hideki Kobara:** Investigation. **Masaki Kamada:** Investigation, Resources. **Kazushi Deguchi:** Resources. **Tetsuo Touge:** Resources. **Tsutomu Masaki:** Resources. **Tohru Yamamoto:** Conceptualization, Methodology, Formal analysis, Investigation, Resources, Writing – original draft, Supervision, Project administration, Funding acquisition.

Declaration of Competing Interest

The authors declare that they have no known competing financial interests or personal relationships that could have appeared to influence the work reported in this paper.

Appendix A. Supplementary data

Supplementary data to this article can be found online at https://doi.org/10.1016/j.brainres.2021.147595.

References

Arakawa, T., Iwashita, M., Matsuzaki, F., Suzuki, T., Yamamoto, T., 2008. Paths, elongation, and projections of ascending chick embryonic spinal commissural neurons after crossing the floor plate. Brain Res. 1223, 25–33. https://doi.org/10.1016/j.brainres.2008.05.062.

Baek, M., Menon, V., Jessell, T.M., Hantman, A.W., Dasen, J.S., 2019. Molecular logic of spinocerebellar tract neuron diversity and connectivity. Cell Rep. 27, 2620–2635.e4.. https://doi.org/10.1016/j.celrep.2019.04.113.

Coughlan, E., Garside, V.C., Wong, S.F.L., Liang, H., Kraus, D., Karmakar, K., Maheshwari, U., Rijli, F.M., Bourne, J., McGlinn, E., 2019. A Hox code defines spinocerebellar neuron subtype regionalization. Cell Rep. 29, 2408–2421.e4.. https://doi.org/10.1016/j.celrep.2019.10.048.

Furue, M., Uchida, S., Shinozaki, A., Imagawa, T., Hosaka, Y.Z., Uehara, M., 2010. Spinocerebellar projections from the cervical and lumbosacral enlargements in the chicken spinal cord. Brain Behav. Evol. 76 (3-4), 271–278. https://doi.org/10.1159/000321910.

Hamburger, H., Hamilton, H.A., 1951. Series of normal stages in the development of the chick embryo. J. Morphol. 88, 49–92. https://doi.org/10.1002/aja.1001950404.

Matsushita, M., Tanami, T., 1987. Spinocerebellar projections from the central cervical nucleus in the cat, as studied by anterograde transport of wheat germ agglutinin-horseradish peroxidase. J. Comp. Neurol. 266 (3), 376–397. https://doi.org/10.1002/cne.902660306.

Okado, N., Ito, R., Homma, S., 1987. The terminal distribution pattern of spinocerebellar fibers. An anterograde labelling study in the posthatching chick. Anat. Embryol. 176, 165–174. https://doi.org/10.1007/BF00310049.

Sagner, A., Briscoe, J., 2019. Establishing neuronal diversity in the spinal cord: a time and a place. Development 146, dev182154. https://doi.org/10.1242/dev.182154.

Sato, Y., Kasai, T., Nakagawa, S., Tanabe, K., Watanabe, T., Kawakami, K., Takahashi, Y., 2007. Stable integration and conditional expression of electroporated transgenes in chicken embryos. Dev. Biol. 305 (2), 616–624. https://doi.org/10.1016/j.ydbio.2007.01.043.

Yaginuma, H., Matsushita, M., 1986. Spinocerebellar projection fields in the horizontal plane of lobules of the cerebellar anterior lobe in the cat: an anterograde wheat germ agglutinin-horseradish peroxidase study. Brain Res. 365 (2), 345–349. https://doi.org/10.1016/0006-8993(86)91647-1.

Watson, C., Harrison, M., 2012. The location of the major ascending and descending spinal cord tracts in all spinal cord segments in the mouse: actual and extrapolated. Anat. Rec. 295, 1683–1691. https://doi.org/10.1002/ar.22547.

Ascending spinal tract formation in chick embryo originating from different spinal regions

Yohei Kokudo[a], Takahiro Arakawa[b], Hiroo Takahashi[b], Hideki Kobara[c], Masaki Kamada[a], Kazushi Deguchi[c], Tetsuo Touge[d], Tsutomu Masaki[c], and Tohru Yamamoto[b*]

[a]Department of Neurological Intractable Disease Research, Faculty of Medicine, Kagawa University, Kagawa 761-0793, Japan
[b]Department of Molecular Neurobiology, Faculty of Medicine, Kagawa University, 761-0793, Japan
[c]Department of Gastroenterology and Neurology, Faculty of Medicine, Kagawa University, Kagawa 761-0793, Japan
[d]Department of Gastroenterology and Neurology, Faculty of Medicine, Kagawa University, Kagawa 761-0793, Japan

* To whom correspondence should be addressed:
 **Tohru Yamamoto** (tohru@med.kagawa-u.ac.jp; +81-87-891-2251)

List of material included:
 Supplemental Figure 1-8 and the figure legends
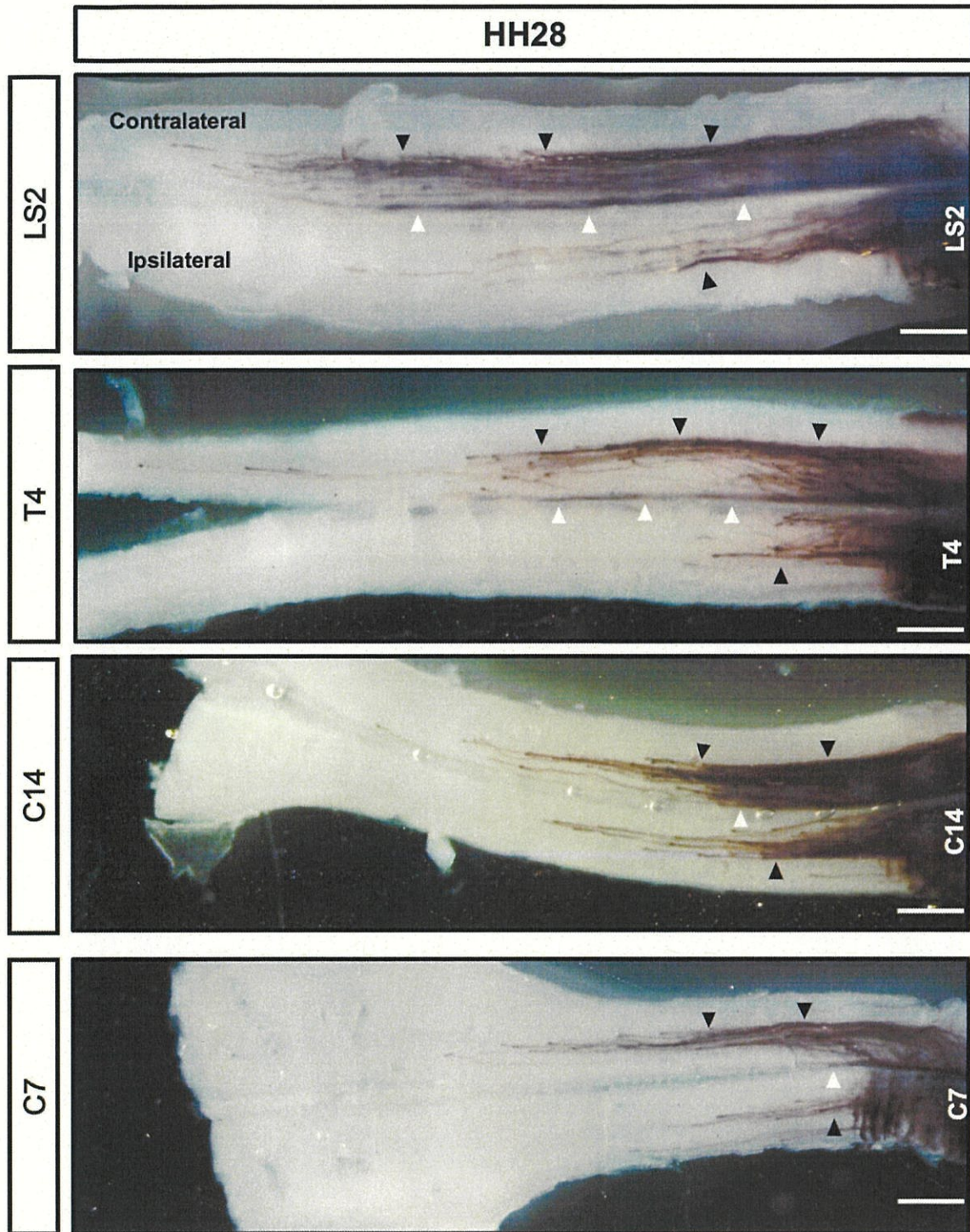
Supplemental Figure 1.
Open-book configuration of HH28 spinal cord, of which ascending axons originating from the indicated spinal segments were visualized. The contralateral side is up, and the ipsilateral side is down. Dorsal paths are indicated by black arrowheads, and ventral paths are indicated by white arrowheads. Scale bar = 0.5mm.
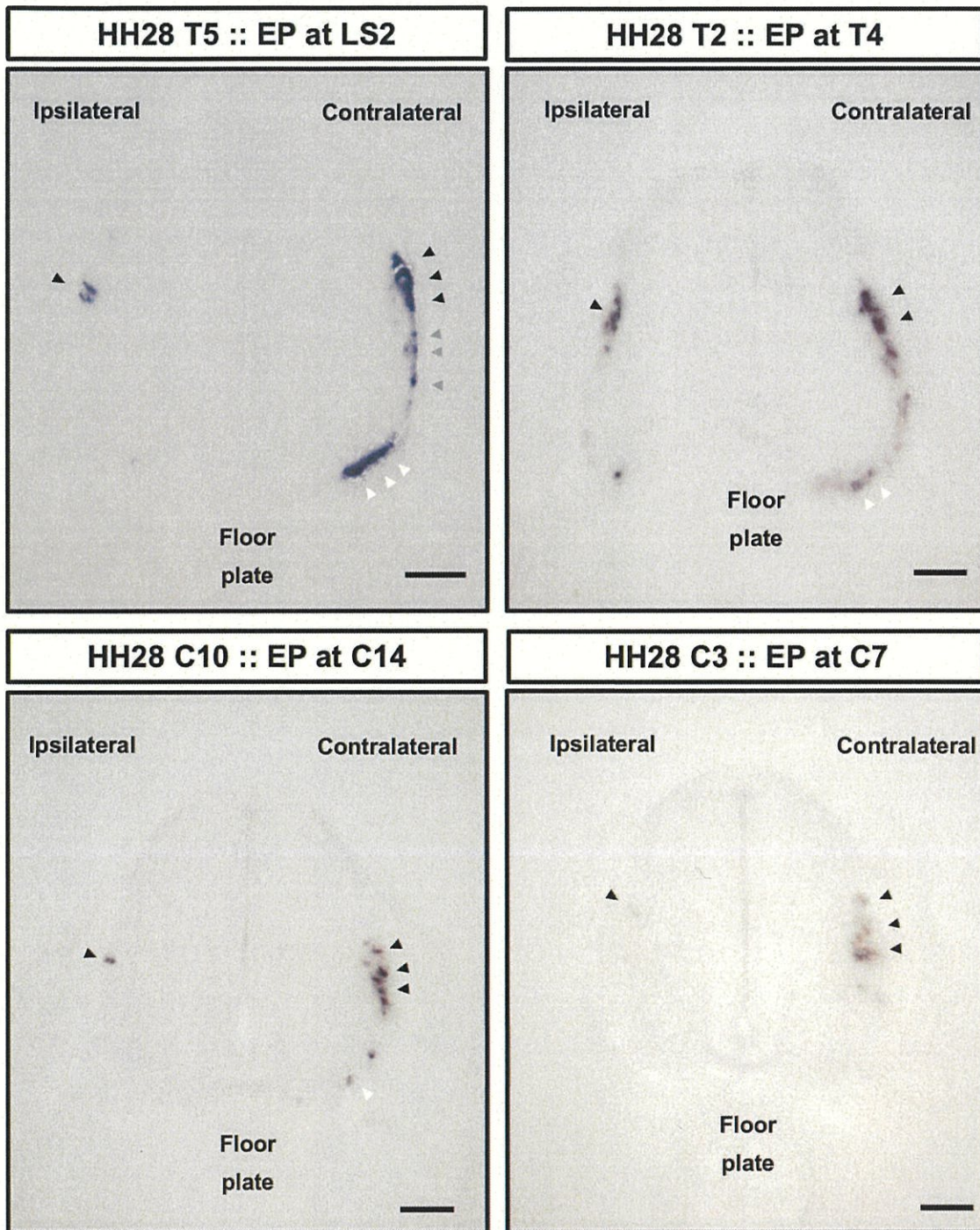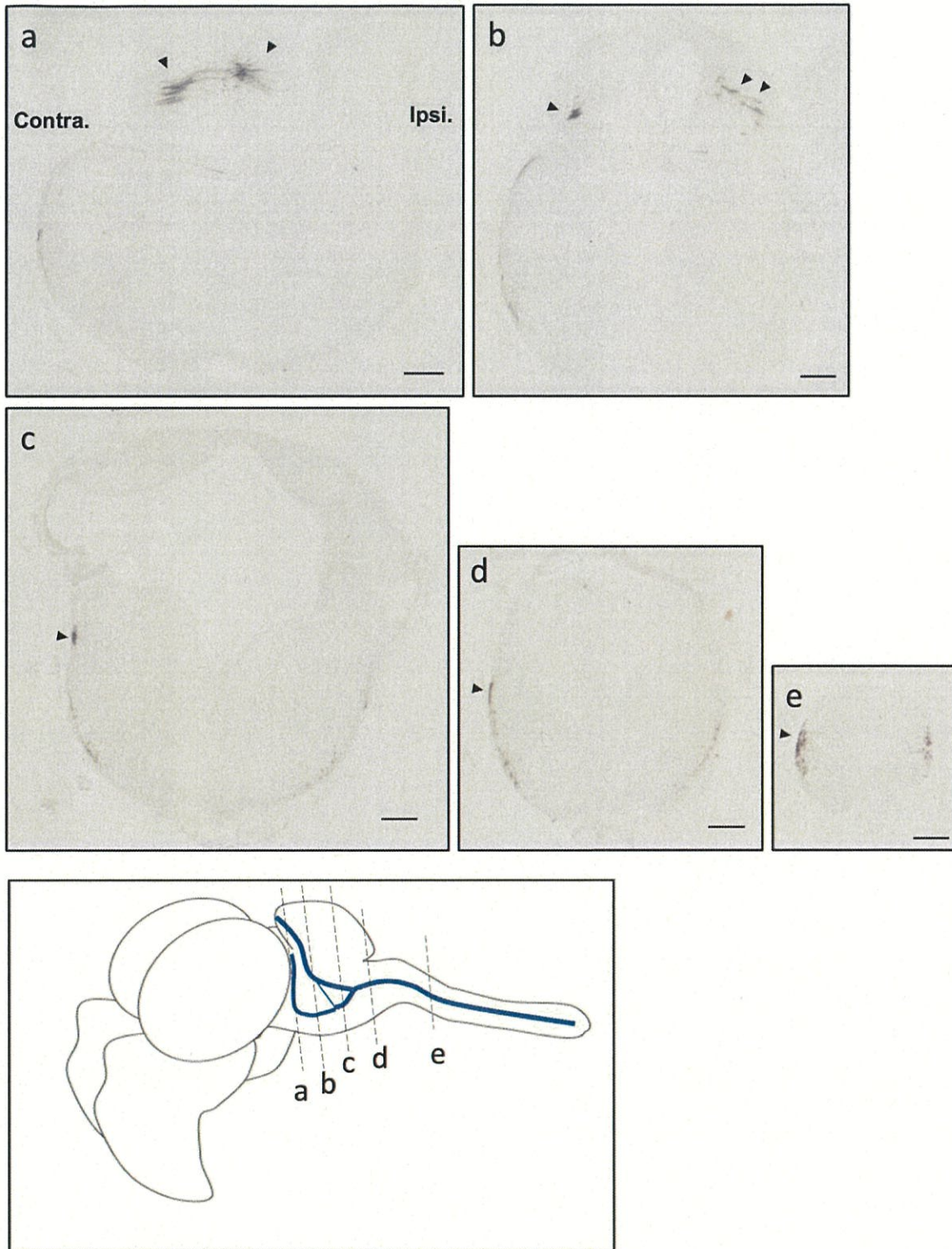
Supplemental Figure 2.
Coronal section of HH28 spinal cords at T5, of which ascending axons originating from LS2; at T2, of which ascending axons originating from T4; at C10, of which ascending axons originating from C14; and at C3, of which ascending axons originating from C7 were visualized. Ipsilateral side is left, and contralateral side is right. Positions of dorsal paths are indicated by black arrowheads, those of ventral paths are indicated by white arrowheads, and those of intermediate paths originating from LS2 are indicated by gray arrowheads. Scale bar = 100μm.
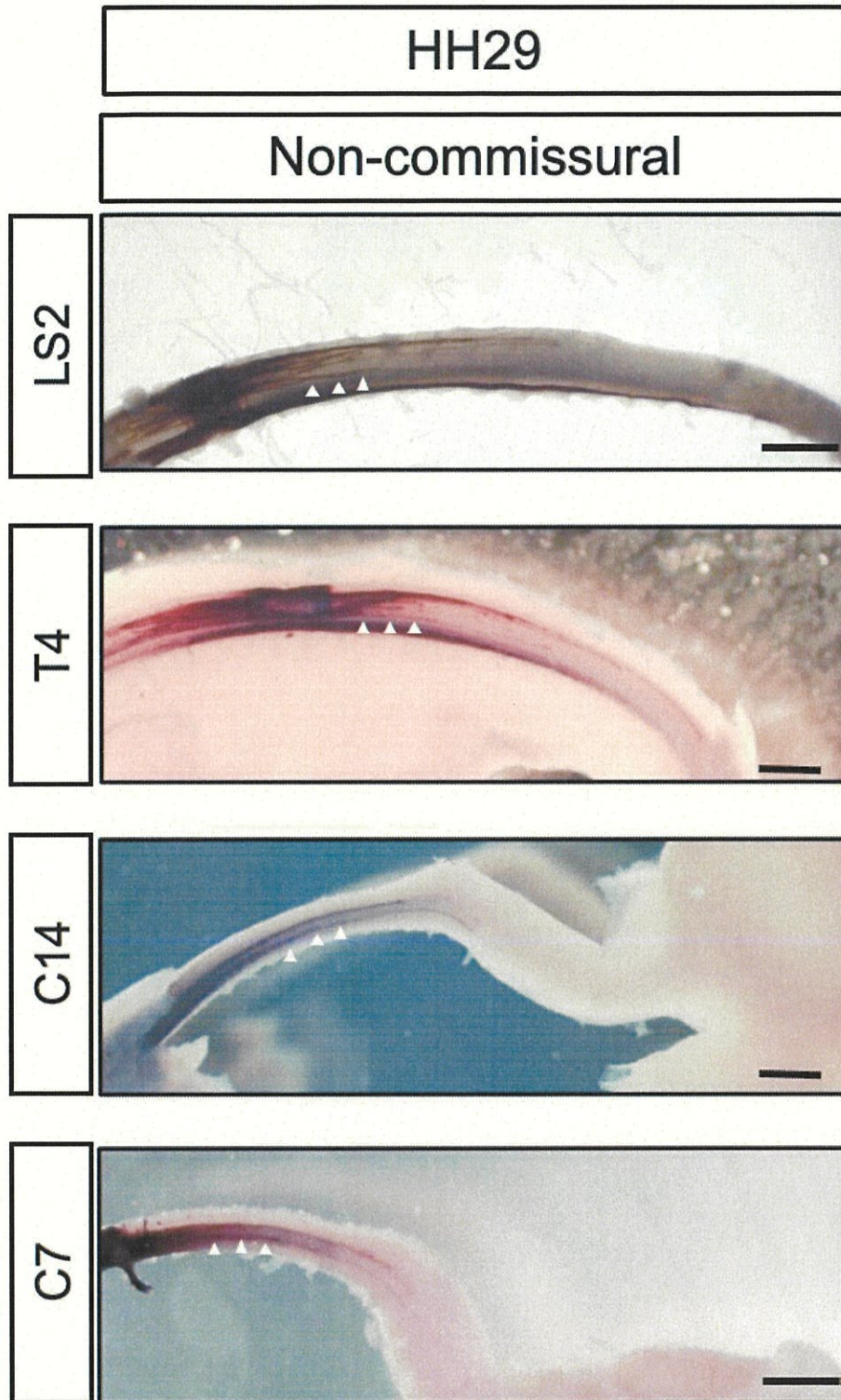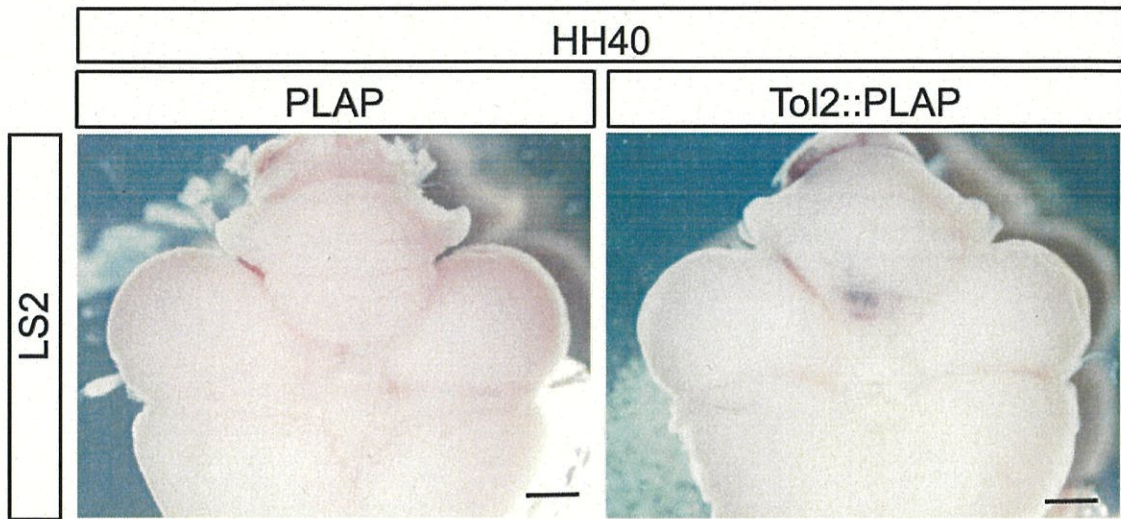
Supplemental Figure 3.
Non-commissural ascending axons originating from LS2, T4, C14, and C7 at HH29. Ventrally running axons are indicated with arrowheads. LS2: n = 7, T4: n = 15; C14: n = 10, C7: n = 4. Scale bar = 1 mm.

Supplemental Figure 4.
Coronal sections of HH35 medulla oblongata with developing cerebellum, of which ascending axons originating from LS2 were visualized. Contralateral side is left, and ipsilateral side is right. Positions of spinocerebellar axons ascending contralateral side are indicated by arrowheads. Scale bar = 300μm.

Supplemental figure 5.
Introduced PLAP activity faded by HH40, which can be extended by Tol2-mediated incorporation of expression vectors. Scale bar = 1 mm.